SAND2021-15358C

Aluminum Combustion in a Shock Tube at High Pressure

Kyle A. Daniel*, Christopher M. Murzyn†, David J. Allen‡,
Kyle P. Lynch†, Charley R. Downing §, Justin L. Wagner¶
Sandia National Laboratories, Albuquerque, NM

This work demonstrates a laser absorption diagnostic capable of measuring the temperature and column density of aluminum monoxide (AlO) at 100 kHz. This diagnostic was fielded in Sandia's High-Temperature Shock Tube (HST) facility, which generated high pressure and temperature environments behind a reflected shock to combust 10-micron diameter aluminum particles. The absorption technique utilized a near infrared microelectromechanical system tunable vertical cavity surface emitting laser (MEMS-VCSEL) capable of sweeping $7,400 - 7,900\mathrm{cm}^{-1}$ and probing the rotationally resolved spectra of the ALO $\mathrm{A}^2\Pi_\mathrm{i} - \mathrm{X}^2\Sigma^+$ transition and atomic aluminum transitions at $7,618\mathrm{cm}^{-1}$ and $7,602\mathrm{cm}^{-1}$. The diagnostic was evaluated at conditions with temperatures and pressures in the range $3200 - 4700$ K and $9 - 64$ Bar. Absorption measurements agree with temperatures estimated from fitted AlO emission spectra for the optically thin case examined. For the high temperature and pressure cases ($\mathrm{T} > 4000$ K, $\mathrm{P} > 60$Bar) the absorption matched the reflected shock temperatures estimated by NASA CEA. These results indicate the laser absorption diagnostic can measure the temperature and column density of AlO in high pressure and temperature environments of high optical thickness where emission spectroscopy may be limited and experimental measurements of aluminum particle combustion remains scarce.

I. Introduction

Metals such as aluminum are often added to propellants to enhance combustion performance in solid rocket motors [1], pulse detonation engines [2], and scramjet systems [3]. As such, a multitude of research has been conducted on aluminum combustion. For instance, it is known that particles in quasi-static environments having diameters $>\sim 20$ μm burn in a diffusion-limited regime, whereas smaller particles (< 10 μm) tend to burn in a transitional regime approaching kinetics-limited combustion [4].

Despite recent progress, gaps in the understanding of particle combustion characteristics at relevant propulsion system conditions remain. As discussed by Glumac et al. [1], the effects of high temperature and pressure may significantly alter combustion behavior and are not well understood. For example, the boiling point of metal and metal oxides increases with pressure. If the boiling point of the particle exceeds the adiabatic flame temperature, a diffusion flame will not be possible. On the other hand, elevated gas temperatures introduce a contrasting effect. The boiling point of aluminum decreases with temperature due to diffusion of oxygen into molten metal [5]. These potentially competing effects make it difficult to elucidate particle combustion behavior at elevated pressure with simultaneous high temperature. To remedy this, an experimental effort using a free-piston shock tube at Sandia National Laboratories is underway to characterize aluminum combustion at elevated temperatures (> 3000 K) and pressures (> 30 bar), where data and viable optical diagnostics remain scarce.

Typically researchers study aluminum combustion using emission spectroscopy to probe the AlO $B^2\Sigma^+ - X^2\Sigma^+$ spectrum, which has a large cross section and is easily accessibly at visible wavelengths. For instance, Ruesch et al. [6] fitted this AlO emission transition for temperature to characterize combustion mechanisms in propellant flames. Lynch et al. [4] used emission to estimate burn times. The authors found the burn time of 3-10 μm particles did not have the strong temperature dependence that is typically observed with nano-sized particles, indicating that the small micron particles studied burn in a transition regime. Using AlO emission data for a range of pressures, temperatures, and oxidizers, the authors generated a burn time correlation for particles in this transition regime. Importantly, these types of correlations have great value to modelers and extend their ability to predict the combustion rates of particles over a range of diameters.

*Postdoctoral Appointee, Member AIAA, kadani@sandia.gov
†Senior Member of the Technical Staff, Engineering Sciences Center, Member AIAA
‡Principal Member of the Technical Staff, Engineering Sciences Center, Member AIAA
§Principal Technologist, Engineering Sciences Center
¶Principal Member of the Technical Staff, Engineering Sciences Center, Associate Fellow AIAA

While extremely useful, quantitative emission spectroscopy measurements have several drawbacks. In combustion environments, light is scattered by condensed phase species and will contaminate emission measurements with information outside of the measurement collection volume. For example, Goroshin et al. [7] attempted to study the thermal structure of an aluminum Bunsen flame using emission spectroscopy. The authors determined the measurements were unreliable as local emission spectra were contaminated from different areas in the flame due to light scattering from particles. Similar light scattering effects were also seen in the emission measurements of Soo et al. [8].

Emission spectroscopy can be complemented by using absorption spectroscopy, which provides an integrated measure of absorption across the path length and is not subject to the scattering effects that plague emission measurements. Further, with an appropriate model, laser absorption measurements can be fit to yield the temperature and the number density of the absorbing molecule. A prominent example of AlO absorption spectroscopy is Glumac et al. [1], who coupled absorption and emission measurements of the $B^2\Sigma^+ - X^2\Sigma^+$ transition to probe the AlO gas phase temperature of 10-μm particles burning in CO_2 at elevated pressure. The authors found fits of both absorption and emission spectra yielded similar temperatures that were well below the adiabatic flame temperature and the boiling temperature of alumina (Al_2O_3). The results from each of these measurements made a strong argument that the particles studied were burning in a kinetic limited combustion regime.

Soo et al. [8] used spatially resolved absorption and emission of atomic aluminum transitions to examine the combustion regime of 2.5-μm particles burning in a flat flame. The authors examined particles burning in stochiometric aluminum-air and methane-air flames. In the case of the air flame, the authors found strong self-reversal of the atomic lines, which indicated high concentrations of aluminum vapor and suggested the particles were burning in a diffusion limited regime. In contrast there was no indication of self-reversal in atomic aluminum transitions for the methane-air flame, suggesting a much smaller amount of aluminum vapor and kinetic limited combustion.

With the notable exception of Glumac et al. [1], almost all absorption spectroscopy measurements of Al or AlO vapor are qualitative [8–11], and primarily use absorption measurements to indicate the presence of vapor phase constituents. This indicates the need for a robust laser absorption measurement that can be used to extract quantitative information from these important aluminum combustion species.

The current study demonstrates the new application of a MEMS-VCSEL absorption diagnostic [12] that is capable of measuring AlO temperature and number density at a 100 kHz repetition rate. Measurements are made of 10-μm aluminum particles combusting in a free-piston shock tube. This study aims to demonstrate the use of the laser absorption diagnostic in high-temperature and pressure environments where gaps in the understanding of particle combustion still exist to enable future physics focused studies.

The remainder of this study is organized as follows: in section II, the shock tube facility and the measurement techniques are described in detail. Section III examines absorbance spectrograms and compares fitted temperatures from absorption and emission spectroscopy to the reflected shock temperature estimated by NASA Chemical Equilibrium with Applications (CEA) code [13]. The results are summarized in Section IV.

II. Experimental Methods

A. High Temperature Shock Tube Facility

The high-temperature shock tube (HST) is a free-piston driven shock tube at Sandia National labs. A shock wave is created by rupturing a diaphragm separating a driven and driver section at different pressures. The HST utilizes isentropic compression to simultaneously pressurize and heat the driver gas, allowing much stronger shock waves to be created compared to traditional shock tubes. The facility is described in more detail in Lynch et al. [14].

The pressure in the driven section is monitored using fast response PCB pressure sensors (113B112). Sensors are provided an excitation voltage and amplified using a PCB model 483C signal conditioner. These voltages are then low-pass filtered using a Krohn-Hite Model 3384 with a four-pole butterworth filter with cutoff frequency of 500 kHz. Data is recorded by an acquisition chassis equipped with a NI PXIe-6376 module that digitizes the signals at a sampling frequency of 2 MHz before being recorded on a personal computer via an in-house LabView code.

Three different cases with varied reflected shock pressures and temperatures were examined. The incident shock Mach number M_s and post-incident and reflected shock conditions of these case are presented in Table 1. Here P_2, T_2 are the post-incident pressure and temperature and P_5, T_5 are the post-reflected pressure and temperature. To generate these conditions a steel diaphragm is burst using various helium-argon mixtures as the driver gas and ambient temperature air as the driven gas.

Post-shock conditions are calculated using the measured incident shock speed as determined by shock crossing times given by the PCB sensors and the initial driven conditions. These values are used as inputs into standard shock tube relations [15] that include real gas effects and are calculated using the NASA Chemical Equilibrium with Applications (CEA) code [13] under the assumption of thermochemical equilibrium following both the incident and

Table 1. Flow Conditions

Case	M_s	u_s (m/s)	p_2 (Bar)	T_2 (K)	p_5 (Bar)	T_5 (K)
1	5.6	1940	1.2	1890	9.2	3210
2	8.2	2810	1.2	3050	11.2	4690
3	6.7	2310	8.0	2450	63.8	4060

reflected shocks. The uncertainty in shock speed, and therefore the post-shock conditions, is determined by applying a uniformly-distributed random uncertainty to the sensor cross time, the bounds of which are defined by the sensor diameter. Variations in shock crossing time for these cases are $\sim$2%.

Aluminum powder with a nominal diameter of $10\mu m$ was loaded into the shock tube using a 0.5 mm diameter, stainless steel rod placed along the same axis as the emission and absorption and offset by 0.2" from the laser path as shown in Fig. 1.

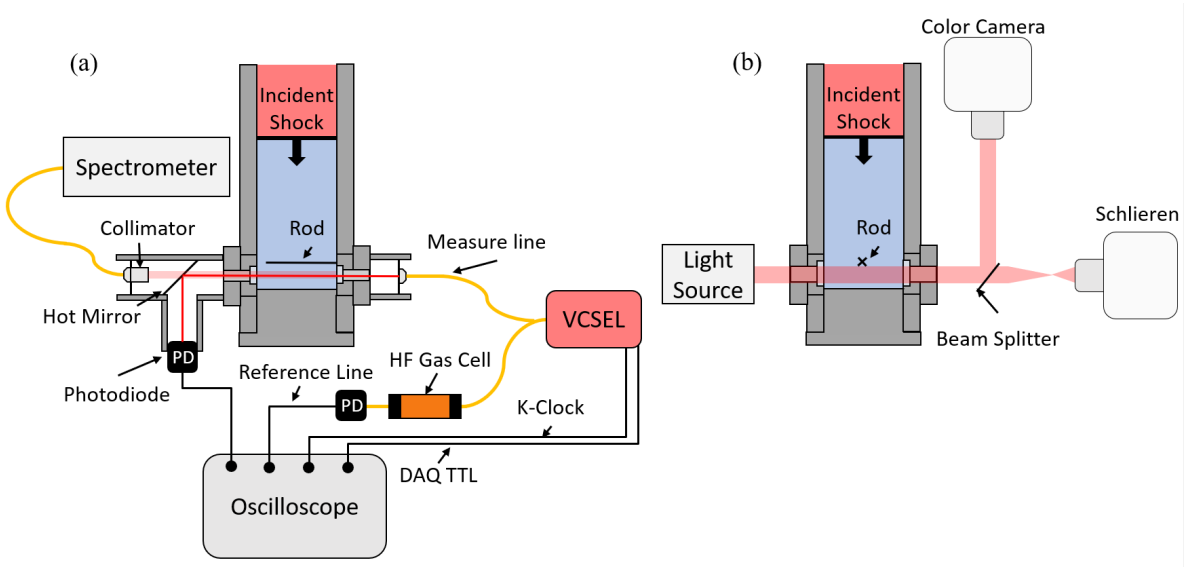

Figure 1. (a) Side view of shock tube test section showing emission collection optics and optical and electrical signal configuration for the laser absorption. (b) Top view of shock tube showing schlieren and color camera fields of view.

B. Flow Visualization

Visualization of the reflected shock wave and the dispersal and combustion of aluminum particles was captured using a lens schlieren system and high-speed color imaging. In the schlieren setup, the light source was a Cavilux Smart pulsed-diode laser with a wavelength of approximately 640 $\pm$ 10 nm. The light was collimated and focused onto the knife edge using two 101.6 mm plano-convex lenses placed on either side of the shock tube test section. A vertical knife edge was used to create schlieren images sensitive to the stream-wise density gradient. Schlieren images were recorded at 450 kHz and at a resolution of 256 x 256 pixels using a Phantom TMX 7510 high-speed video camera. The light generated by the emission of shock heated air and the luminescence of burning aluminum was filtered from the schlieren images using a 640 $\pm$ 10 nm band pass filter. The luminescence of burning aluminum particles was examined using a Phantom V1212 color camera. Color images were recorded at 100 kHz at a resolution of 250 x 250 pixels. Schlieren and color imaging measurements viewed the aluminum loading rod through the same window port and were taken simultaneously with LAS and emission measurements.

The dispersal and combustion of aluminum particles are captured by the schlieren and color images in Fig. 2. Here the vertical red line represents the collection volume of the LAS and emission measurements respectively. The formation of the reflected shock is set as times t=0μs. In Fig 2a,e, the reflected shock has formed and passed over the aluminum loading rod as is travels towards the left hand side of the image. Here particles have just begun to disperse

from the loading rod and are in the intial stages of combustion, as shown by the dim flame structure in Fig 2e. At later time steps in Figs. 2(b,e,f,g), particles continue to disperse from and move into the path the LAS and emission measurements. The combustion of the particles can be observed by the bright blue color in Fig. 2(f,g) and by the white emission in the schlieren image in Fig. 2(c). This process continues in Fig. 2(d,h), as the intense light from burning particles saturates the color camera.

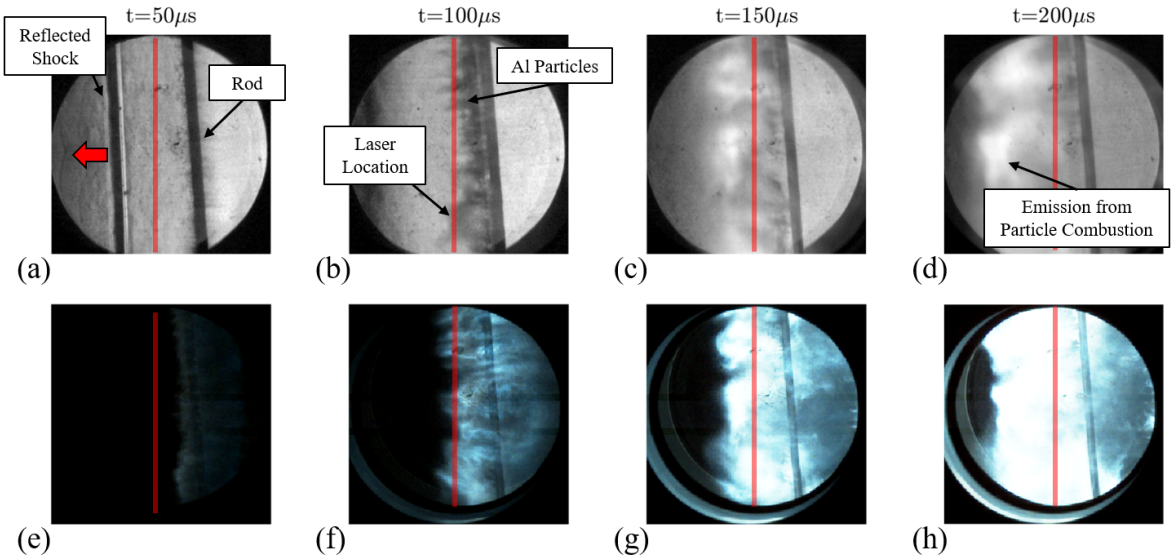

Figure 2. Schlieren (a-d) and color camera (e-h) images of aluminum particle combustion at multiple time steps. The reflected shock moves right to left and the red line represents the location of the LAS laser and emission field of view. The reflected shock is formed at time t= 0μs.

C. Laser Absorption Spectroscopy

Near infrared (NIR) laser absorption spectroscopy (LAS) of AlO $A^2\Pi_i - X^2\Sigma^+$ transition is a recent diagnostic development that enables high precision quantification of AlO temperature and number density at a 100 kHz repetition rate [12]. The technique utilizes a wavelength-agile MEMS-VCSEL (Thor Labs: SL131090), which scans from 1265 to 1351 nm (7400-7900cm^{-1}) at a rate of 100$cm^{-1}/\mu s$ when run with a 70 % duty cycle.

The original demonstration of this technique was probing an isobaric aluminum combustion event at a standard Albuquerque atmosphere. The present work significantly advances the state-of-the-art by expanding the capability to include combustion problems at elevated temperatures and pressures.

Data was collected using a four-channel scheme described in Fig 1. The optical power from the laser was split using a 90:10 fiber (Newport: F-CPL-B12351-FCUPC), with 90% of the laser power going to the absorption measurement and the remaining 10% used in a wavelength reference channel. In the measurement channel, the laser is transmitted across the shock tube test section and collected using an InGasAs photodiode with 5 GHz (-3dB) bandwidth (Thor Labs: DET08CL) and recorded using an oscilloscope operating with a 4GHz bandwith, 12-bit resolution at 12.5 GS/s (Textronix: MS064B). The wavelength reference consisted of hydrogen fluoride (HF) gas cell (Wavelength References: HF-C(2.7)-50) comprised of a 100% HF at 50 Torr with a path length of 2.7 cm. The laser energy passed through the HF Cell, was collected using a photodiode (Thor Labs: DET08CFC), and recorded on a separate oscilloscope channel. This channel yielded narrow absorption features spanning the spectral tuning range and was collected simultaneously with the laser absorption measurement. A relative wavenumber axis was found using the VCSEL's k-clock channel, which is a 900 MHz digital signal generated from a Mach-Zehnder interferometer. The last channel was a DAQ TTL pulse, generated by the VSCEL at the beginning of each laser sweep. The wavelength reference, k-clock channel, and DAQ TTL pulse are used in post processing to discretize the continuous signal from the oscilloscope and generate time resolved absorption spectra.

Although the laser absorption hardware required no modification for studying higher pressure combustion, the data reduction via model fitting had to be expanded to include the observed pressure broadening effects on spectroscopic lineshapes. At the time of this report, there are no line broadening models specific to AlO available in the literature.

Instead, pressure broadening was estimated using Sandia's spectral modeling application programing interface (API) that integrates a hard sphere collisional model to calculate the Lorentz component of the Voigt function [16]. In short, the API was used to generate a look up table of AlO cross sections as a function of temperature and collisional width. A Nelder-Mead optimization algorithm then minimizes the residual between a measured spectrum and the entries in the table. Although 600 cm^{-1} was measured in each laser sweep, models were regressed over the 7,400-7,480 cm^{-1} range. This generalized approach allowed data collected across a wide range of pressure broadened lineshapes to be fit without needing an explicit model for collisional width at a given pressure. This process is analogous to floating the Lorentz component of the Voigt profile. Example results from model fits at multiple time steps are shown in Fig. 3.

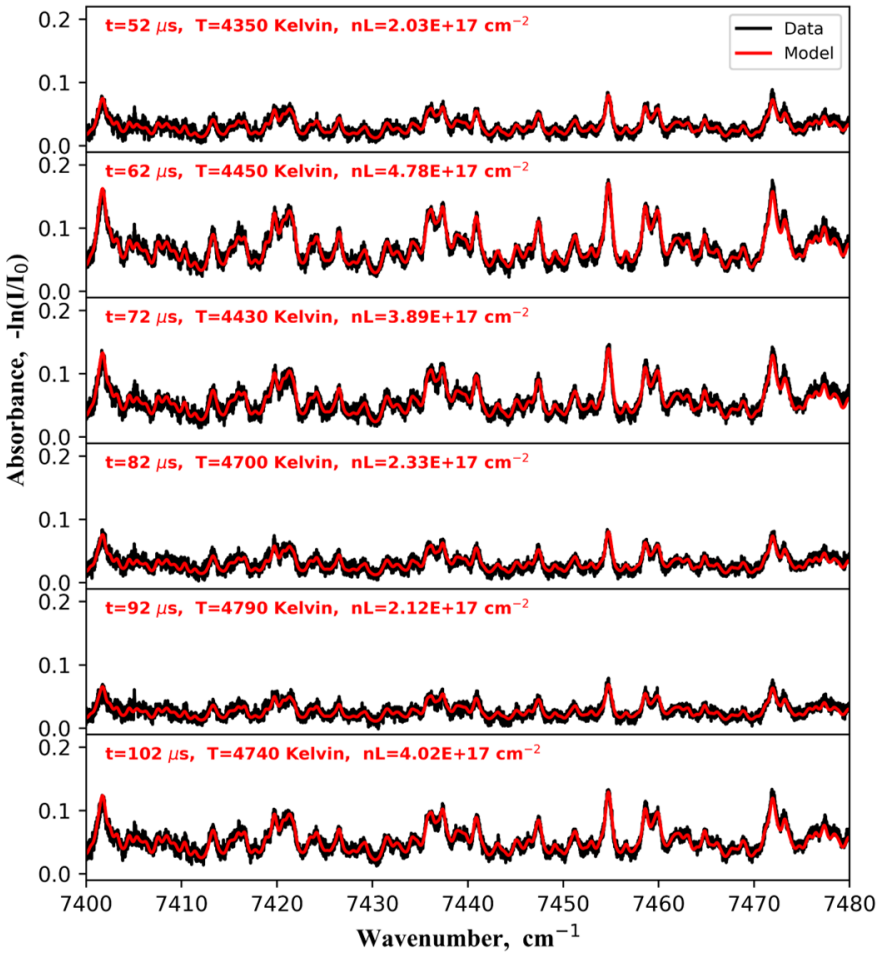

Figure 3. Comparison of measured VCSEL absorbance spectra and aluminum monoxide model regressions for multiple time steps in case 2.

D. Emission Spectroscopy

Emission spectra were taken at 11 kHz using a Princeton Instruments ProEM HS: 1024BX3 camera and a Horiba iHR320 spectrometer. Light was collected from the shock tube using a doublet collimator rigidly attached to the shock tube. Note the collection path of the emission was colinear with LAS measurements as shown in Fig. 1. Collected light was sent through a 1500 μm diameter multimode fiber and focused into the spectrometer slit using a 12 mm reflected collimator and a 100 mm lens.

The emission spectrometer was calibrated for wavelength over the range of 525-555 nm using a neon pen lamp by linearly regressing the wavelengths of the identified peaks. In addition the neon lines were fit assuming a gaussian function to determine an instrument broadening function. This instrument function determined to have an optimized FWHM of 0.09 nm and this was subsequently propagated into the spectral model for fitting the Δv=-2 band of AlO B-X emission.

The look up table of instrument-degraded cross sections was again calculated using the SNL spectral modeling API [16]. The model included a condensed phase emissive contribution assumed to be both gray and at the same temperature as the gas phase AlO. The quality of fits shown in Fig. 4 suggest these assumptions are good across our limited spectral range and at the temperatures and pressures tested in the present work. These assumptions may break down over wider spectral ranges of different combinations of temperature and pressure. The model also allowed for a variable optical depth to accommodate the optically thick spectra observed in some tests. In addition there was a scaling parameter and a constant value relative shift parameter implicit to the fitting procedure to scale and shift model and experiment relative intensities.

The spectral model for the AlO B-X was derived from ExoMol spectral data for AlO [17]. It was noticed that a sharp drop in emissive intensity was observed in the spectral region immediately prior to the Δv=-2 bandhead (532 - 533 nm). It is suspected that this may be due to a lack of inclusion of higher J rotational values in the Exomol data base which would contribute to emission at the tail end of the AlO Δv=-1 band. A more recent line list has been incorporated into Exomol [18] and may improve in this area but this has not been investigated to date. The wavelengths between 532-533 nm were ignored in the residual calculation of the parameter optimization routine.

The uncertainty in the emission measurements has previously been estimated at $\pm$150 K [1]. The spectral resolution in the work by Glumac et al. [1]. was greater than that in the emission measurements obtained here. With the decrease in spectral resolution we expect our temperature sensitivity to be reduced and conservatively place it at $\pm$250 K based upon residual variance in our temperature and emissivity fitting optimization. In addition the larger uncertainty is due to the greater optical depths that were observed in some of the measurements. Increasing optical depth has an effect on the spectrum similar to that of increasing the temperature and therefore the uncertainty in the fits is greater. In the work by Glumac et al. [1]. fits were only performed on the spectrum if the optical depth was less than 1. The emission temperature fit has significantly larger uncertainty in comparison to the recently developed laser absorption technique. This is in large part due to the laser absorption technique resolving the true lineshape of the AlO species while the emission technique is largely instrument broadened.

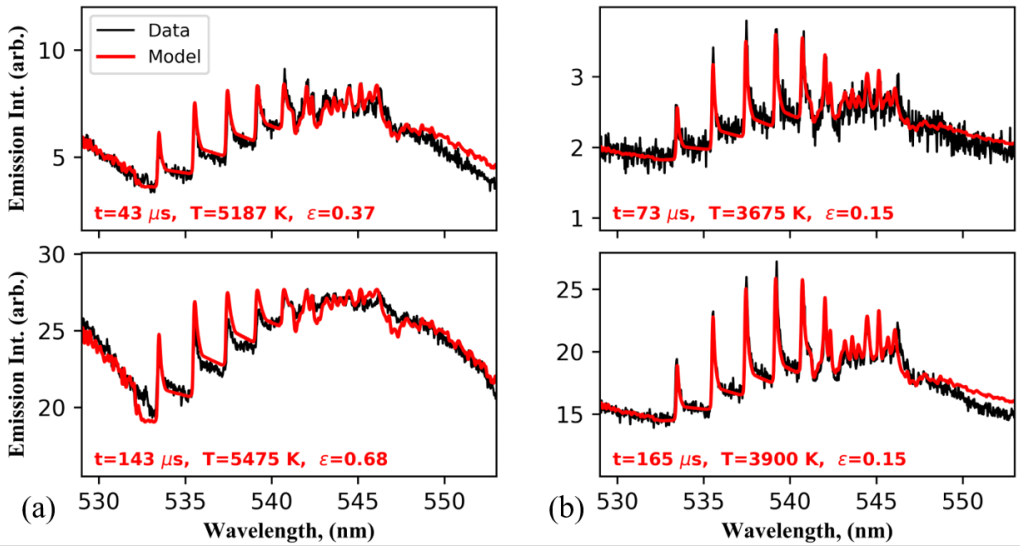

Figure 4. Comparison of measured AlO emission spectra with model fit for (a) case 2 and (b) case 1.

III. Results & Discussion

The wide scanning range and 100 kHz repetition rates of the LAS diagnostic enables the time resolved evolution of AlO and Al absorption to be studied. The spectrograms in Fig. 5 depict the temporal changes in Al and AlO absorption for the cases listed in Table 1. Case 1 (Fig. 5a) represents a similar ambient pressure and slightly higher temperature (T=3200 K, P=9 Bar) compared to conditions studied in the literature [1, 4, 19]. Here a small amount of AlO absorbance is observed 200-500μs after the reflected shock, indicating an ignition delay of $\sim$200μs. This agrees with ignition delays observed by Servaites et al. [20] at similar conditions. Note the uniform region of high absorbance at $\sim$180μs represents measurement times when the particle cloud blocked the laser.

The last two cases evaluated the LAS diagnostic at extremely high temperature and pressure. The spectrogram from the high temperature case 2 (T=4700 K and P=11 Bar) in Fig. 5b shows very strong absorption of Al and AlO $\sim$50μs after the reflected shock. Note the change of color bar axis between Figs. 5a,c and 5b. In the high pressure case 3 (T=4000 K, P=64 Bar), the AlO and Al vapor is again present at early times, appearing $\sim$50μs after the reflected shock. The level of Al absorption here is much lower compared to case 2 and the AlO absorption features are blurred due to pressure broadening.

The observed trends in the spectrograms suggest changes in the combustion behavior over the range of conditions studied. As the temperature increases from T=3100 K to 4700 K, the degree of Al absorption increases and the ignition delay time decreases from $\sim$200μs to 50μs. Physical interpretation of these results is complicated by the the high ambient temperatures examined, which are greater than the volatilization temperature of Al_2O_3 (T >4000 K). In these high temperature environments it is unclear if Al_2O_3 is volatilizing and reacting as a gas or reacting at the surface and producing gas phase Al.

Although questions on the present aluminum combustion mechanisms remain, the capability of the LAS diagnostic over a wide range of extreme test conditions is shown here. The spectrograms in Fig. 5 demonstrate the LAS can measure time-resolved absorption spectra of both Al and AlO vapor over a range of temperatures and pressures and can be used to estimate ignition delay and total burn times. Given this capability the diagnostic has potential for future physics focused experiments, particularly at high pressure conditions where gaps in the fundamental understanding of particle combustion remain.

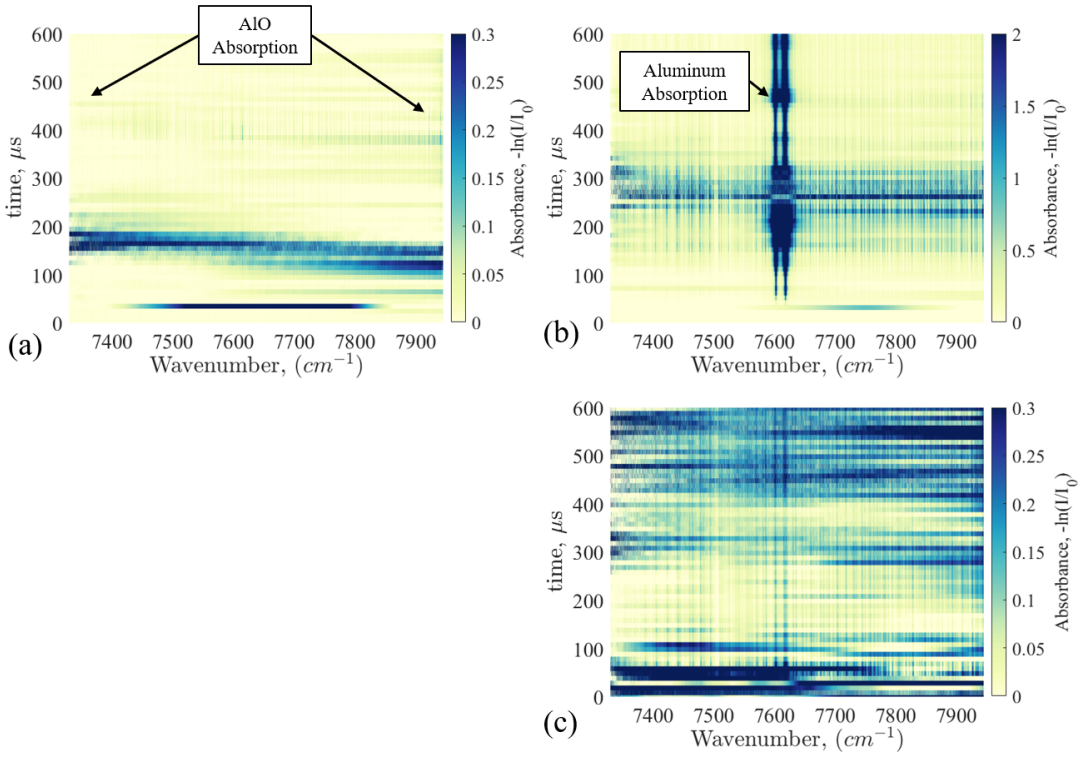

Figure 5. Spectrograms of measured absorbance for case 1 (a), case 2 (b), and case 3 (c). Note different color axis on (b). Here a time of $t = 0$ is when the reflected shock forms.

A time resolved measure of the temperature and number density of AlO from the LAS diagnostic are plotted in Fig. 6. Here, LAS fitted temperatures are compared to temperatures from emission fits, CEA estimated reflected shock temperatures, and the endwall pressure trace. For the CEA reflected shock temperature, the transparent gray area is the temperature uncertainty related to the measured shock speed.

In case 1 (T=3200 K, P=9 Bar), the LAS temperature is $\sim$400 K higher than the CEA estimated temperature and stays relatively constant up until $\sim$350μs, where it increases from 3550K to 3890K. The endwall pressure trace is flat up until $\sim$350μs, after which the pressure begins to rise. This pressure rise is related to compression waves produced

by the contact surface-reflected shock interaction that enters the test section. The slight increase in LAS temperature may be related to the temperature rise associated with the compression wave. The LAS measure of column density indicates the concentration of AlO remains relatively constant and then increases dramatically at ∼350 μs. Schlieren imaging suggest the increase in column density is related to additional burning particles entering the LAS collection volume.

The emission temperature agrees with the LAS measurement when the uncertainty in the emission temperature ($\sim \pm 250$ K) is considered. The temperatures measured by the emission and LAS are higher than the CEA estimated ambient temperature, suggesting diffusion limited combustion. The 10-μm particles used in this study have been previously been shown to burn in the transition region from diffusive to kinetic limited combustion. Particles with diameters <20μm will burn in a diffusion limited regime and begin to approach kinetic limited combustion as the diameter decreases [21]. Therefore it is reasonable to conclude that the LAS and emission temperature measurements are of AlO in a diffusion diffusion flame, where temperatures will be grater than the ambient.

In the high temperature case 2 (T=4700 K and P=11 Bar) the LAS temperature matches the ambient temperature. The column density is approximately constant until ∼110μs where it then increases monotonically. Schlieren images of these times indicate the increase in column density is related to additional aluminum particles leaving the loading rod and entering the LAS measurement volume. The emission temperature for the case is much higher than the ambient and the LAS prediction and is likely due to emission spectrum being optically thick [1, 22]. Case 3 tests the LAS diagnostic at extremely high pressures (T=4000 K, P=64 Bar) where significant lineshape broadening occurs. In this case, the fits of the LAS measurement yield temperatures that match the ambient.

In cases 2,3, the reflected shock temperature is above the volatilization temperature of Al_2O_3, meaning the maximum temperature of the system will be the reflected shock temperature. Therefore at these conditions, the AlO temperature will be at the reflected shock temperature, which is consistent with the LAS measurements.

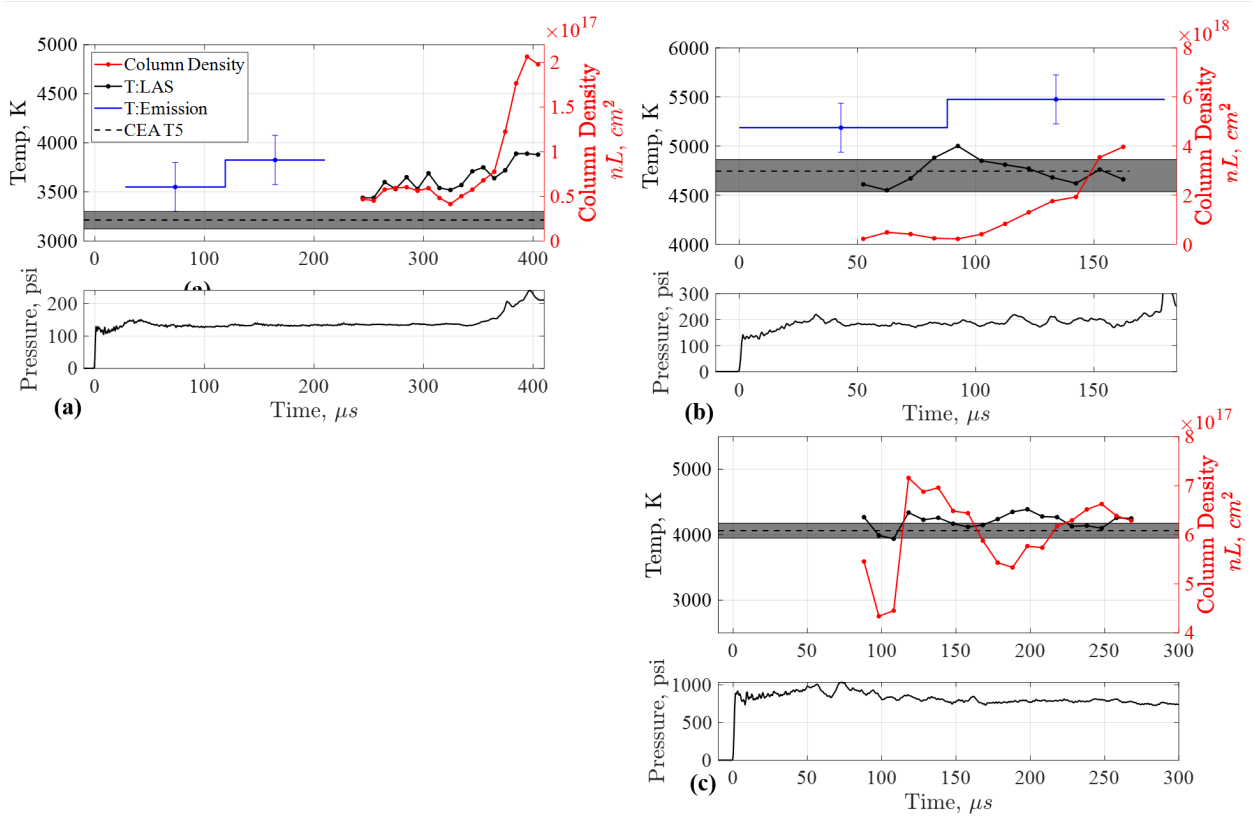

Figure 6. Comparison of time-resolved LAS measurements of column density and temperature with fitted emission temperatures and CEA predicted reflected shock temperature. Gray area around CEA temperature represents temperature variation due to uncertainty in measured shock speed. Temperature and column density compared to endwall pressure trace for case 1 (a), case 2 (b), and case 3 (c).

IV. Conclusion

This work presents simultaneous laser absorption, emission, schlieren and color imaging measurements of aluminum combustion at high temperatures and pressures in Sandia's High Temperature Shock tube. The laser absorption diagnostic developed is capable of measuring the temperature and column density of AlO at 100kHz [12]. The diagnostic utilizes a near infrared MEMS VCSEL to measure the AlO $A^2\Pi_i - X^2\Sigma^+$ transition and atomic Al transitions at 7,618 cm^{-1} and 7,602 cm^{-1}. AlO is produced by the combustion of 10-μm aluminum particles in environments with temperatures and pressures in the range 3000-4700 K and 9-66 Bar.

Spectrograms of the absorption show a decrease in the ignition delay time and increase in the strength of the Al absorption as the ambient temperature increases from T=3000 K to 4700 K. The temperature fits of the AlO absorption agree with the AlO emission temperature fits for an ambient temperature $T = 3100$. For the higher temperature and pressure cases ($T >$4000 K, $P >$60 bar), the emission becomes optically thick and overestimates the AlO temperature, wheras the LAS measurement matches the CEA estimated reflected shock temperature. Column density measurements of AlO are reported and show trends consistent with observations from schlieren images, i.e., as additional aluminum particles are observed moving into the LAS measurement volume the measured column density increases. These results suggest the presented laser absorption diagnostic can accurately measure temperature in high temperature and pressure environments where emission spectroscopy may fail due to optical thickness limitations.

Acknowledgments

Sandia National Laboratories is a multi-mission laboratory managed and operated by National Technology and Engineering Solutions of Sandia, LLC., a wholly owned subsidiary of Honeywell International, Inc., for the U.S. Department of Energy's National Nuclear Security Administration under contract DE-NA0003525.

This work is supported by the Laboratory Directed Research and Development (LDRD) program at Sandia National Laboratories.

References

[1] Glumac, N., Krier, H., Bazyn, T., and Eyer, R., "Temperature measurements of aluminum particles burning in carbon dioxide," *Combustion science and technology*, Vol. 177, No. 3, 2005, pp. 485–511.

[2] Palaszewski, B., Jurns, J., Breisacher, K., and Kearns, K., "Metallized gelled propellants combustion experiments in a pulse detonation engine," *40th AIAA/ASME/SAE/ASEE Joint Propulsion Conference and Exhibit*, 2006, p. 4191.

[3] Rathi, N. and Ramakrishna, P., "Attaining hypersonic flight with aluminum-based fuel-rich propellant," *Journal of Propulsion and Power*, Vol. 33, No. 5, 2017, pp. 1207–1217.

[4] Lynch, P., Krier, H., and Glumac, N., "A correlation for burn time of aluminum particles in the transition regime," *Proceedings of the Combustion Institute*, Vol. 32, No. 2, 2009, pp. 1887–1893.

[5] Dreizin, E. L., "Experimental study of stages in aluminium particle combustion in air," *Combustion and Flame*, Vol. 105, No. 4, 1996, pp. 541–556.

[6] Ruesch, M. D., McDonald, A. J., Mathews, G. C., Son, S. F., and Goldenstein, C. S., "Characterization of the influence of aluminum particle size on the temperature of composite-propellant flames using CO absorption and AlO emission spectroscopy," *Proceedings of the Combustion Institute*, Vol. 38, No. 3, 2021, pp. 4365–4372.

[7] Goroshin, S., Mamen, J., Higgins, A., Bazyn, T., Glumac, N., and Krier, H., "Emission spectroscopy of flame fronts in aluminum suspensions," *Proceedings of the Combustion Institute*, Vol. 31, No. 2, 2007, pp. 2011–2019.

[8] Soo, M., Goroshin, S., Glumac, N., Kumashiro, K., Vickery, J., Frost, D. L., and Bergthorson, J. M., "Emission and laser absorption spectroscopy of flat flames in aluminum suspensions," *Combustion and Flame*, Vol. 180, 2017, pp. 230–238.

[9] Glumac, N., "Absorption spectroscopy measurements in optically dense explosive fireballs using a modeless broadband dye laser," *Applied spectroscopy*, Vol. 63, No. 9, 2009, pp. 1075–1080.

[10] LoCurto, A. C., Welch, M. A., Sippel, T. R., and Michael, J. B., "High-speed visible supercontinuum laser absorption spectroscopy of metal oxides," *Optics Letters*, Vol. 46, No. 13, 2021, pp. 3288–3291.

[11] Lynch, P., Fiore, G., Krier, H., and Glumac, N., "Gas-phase reaction in nanoaluminum combustion," *Combustion science and technology*, Vol. 182, No. 7, 2010, pp. 842–857.

[12] Murzyn, C., Allen, D., Baca, A., Ching, M., and Marinis, R., "Tunable Infrared Laser Absorption Spectroscopy of Aluminum Monoxide $A^2\Pi_i$ $X^2\Sigma+$," *Journal of Quantitative Spectroscopy and Radiative Transfer*, Vol. accepted manuscript, 2022.

[13] "NASA. [Online]. Available: https://www.grc.nasa.gov/www/CEAWeb/ceaHome.htm," .

[14] Lynch, K. P. and Wagner, J. L., "A free-piston driven shock tube for generating extreme aerodynamic environments," *AIAA Scitech 2019 Forum*, 2019, p. 1942.

[15] Anderson, J. D., *Modern compressible flow: With Historical Perspective*, McGraw-Hill Education, 2003.

[16] Murzyn, C., Jans, E., and Clemenson, M., "SPEARS: A Database-Invariant Spectral modeling API," *Journal of Quantitative Spectroscopy and Radiative Transfer*, Vol. 277, 2022, pp. 107958.

[17] Patrascu, A. T., Yurchenko, S. N., and Tennyson, J., "ExoMol molecular line lists – IX. The spectrum of AlO," *Monthly Notices of the Royal Astronomical Society*, Vol. 449, No. 4, 04 2015, pp. 3613–3619.

[18] Bowesman, C. A., Shuai, M., Yurchenko, S. N., and Tennyson, J., "A high-resolution line list for AlO," *Monthly Notices of the Royal Astronomical Society*, Vol. 508, No. 3, 09 2021, pp. 3181–3193.

[19] Bazyn, T., Krier, H., and Glumac, N., "Oxidizer and pressure effects on the combustion of 10-micron aluminum particles," *Journal of propulsion and power*, Vol. 21, No. 4, 2005, pp. 577–582.

[20] Servaites, J., Krier, H., Melcher, J., and Burton, R., "Ignition and combustion of aluminum particles in shocked H2O/O2/Ar and CO2/O2/Ar mixtures," *Combustion and flame*, Vol. 125, No. 1-2, 2001, pp. 1040–1054.

[21] Bazyn, T., Krier, H., and Glumac, N., "Evidence for the transition from the diffusion-limit in aluminum particle combustion," *Proceedings of the Combustion Institute*, Vol. 31, No. 2, 2007, pp. 2021–2028.

[22] Peuker, J. M., Lynch, P., Krier, H., and Glumac, N., "On AlO emission spectroscopy as a diagnostic in energetic materials testing," *Propellants, Explosives, Pyrotechnics*, Vol. 38, No. 4, 2013, pp. 577–585.